

Extracting polygonal footprints in off-nadir images with Segment Anything Model

Kai Li^{a,b,c}, Jingbo Chen^a, Yupeng Deng^a, Yu Meng^{a,*}, Diyou Liu^a, Junxian Ma^{a,c}, Chenhao Wang^{a,c}

^a Aerospace Information Research Institute, Chinese Academy of Sciences, Beijing 100101, China

^b School of Data Science, City University of Hong Kong, Hong Kong 999077, China

^c School of Electronic Electrical and Communication Engineering, University of Chinese Academy of Sciences, Beijing 100049, China

Abstract

Building Footprint Extraction (BFE) in off-nadir aerial images often relies on roof segmentation and roof-to-footprint offset prediction, then drugging roof to footprint via the offset. However, the results from this multi-stage inference are not that applicable in data production, because of the low quality of masks given by prediction. To solve this problem, we proposed OBMv2 in this paper, which supports both end-to-end and promptable polygonal footprint prediction. Different from OBM, OBMv2 using a newly proposed Self Offset Attention (SOFA) to bridge the performance gap on bungalow and skyscraper, which realized a real end-to-end footprint polygon prediction without postprocessing. Additionally, to squeeze information from the same model, we were inspired by Retrieval-Augmented Generation (RAG) in Nature Language Processing and proposed "RAG in BFE" problem. To verify the effectiveness of the proposed method, experiments were conducted on open datasets BONAI and OmniCity-view3. A generalization test was also conducted on Huizhou test set. The code will be available at <https://github.com/likaiucas/OBM>.

Keywords: Building footprint extraction, building detection, Segment Anything Model (SAM), Offset-Building Model (OBM), off-nadir aerial image, Nadaraya-Watson regression, look-ahead masking

1. Introduction

Building Footprint Extraction (BFE) problem has been studied over a decade, which is a fundamental task for 3D building reconstruction, building change detection and so on. In the early stage, building related problems were often studied by using machine learning based methods (Inglada, 2007) or geometric features (Lafarge et al., 2010; Ortner et al., 2008). These methods often limited by conditions like shallow features, demanding human measuring, poor generalization and so on.

With the turn-up of Deep Convolutional Networks, offset-based methods became a popular solutions for BFE problems (Christie et al., 2020; Li et al., 2021; Wang et al., 2023a; Li et al., 2024b,a), and has be-

come a promising and cost-efficient solution for solving BFE problem. Offset-based methods can solve BFE problem in off-nadir images which can easily derived by a satellite camera with a shooting angle. This data requirement, not angle demanding, brings lower data acquisition cost and larger data coverage compared to methods using LiDAR data (Priestnall et al., 2000; Khattak et al., 2013; Kunwar et al., 2021; Lian et al., 2021).

There are some limitation in current offset-based methods. Christie et al. (2020) proposed a method uses a U-Net decoder with a ResNet encoder to predict the image-level orientation and per-pixel height values. Lastly, the orientation and pixel-level height values are multiplied to get the final flow offsets. However, this method only focuses on single-task height estimation with demanding training prerequisites. Aiming at solving this prerequisite, Li et al. (2021) proposed a multi-task learning model, namely MTBR-Net, to facilitate the learning progress. MTBRNet includes an image-wise offset angle prediction task and two pixel-wise offset field prediction tasks, as well as

*Yu Meng is the corresponding author.

This research was funded by the National Key R&D Program of China under Grant number 2021YFB3900504.

Here is information on the communication with Kai Li, which will be interact with the journal editors. likai211@mails.ucas.ac.cn

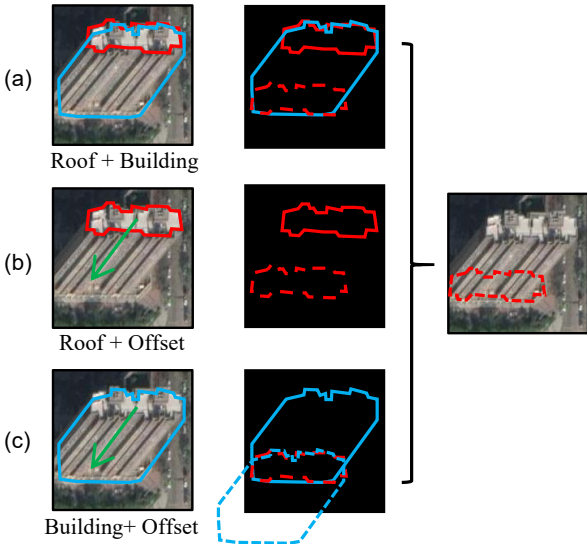


Figure 1: This figure illustrates how to search building footprints with limited information. In (a), with roof segmentation and building segmentation, we find a path on the building map via which roof can find a place better fitting the footprint. In (b), building footprint was derived by dragging roof via the offset. In (c), dragging building segmentation via the offset and the union of both masks represents building footprint. If building segmentation moved in opposite direction, the union can represent the roof segmentation.

several semantic-related tasks. In 2023, Wang et al. (2023a) proposed an instance-level model, LOFT, which was designed based on Mask RCNN (He et al., 2017). This model simplified the multi-task training labels. LOFT leverages an offset Region of Interest (ROI) head to extract roof-to-footprint offsets for each instance building nominated by Region Proposal Network (RPN). The final footprint masks were derived by dragging the predicted roofs to their footprints via the offsets. However, the cost of annotating remote sensing images with offsets is still high, which cannot be trained with diverse labels. In order to train model with offset-unknown samples, Li et al. (2024b) proposed a Multi-Level Supervised Building Reconstruction Network (MLS-BRN) based on LOFT. MLS-BRN added four additional tasks compared with LOFT: (1) off-nadir angle prediction task; (2) offset angle prediction task; (3) footprint segmentation task; (4) real-world height prediction task.

However, those ROI-based methods can hardly applied in real data production because of unstable RPN and Non-Maximum Suppression (NMS) algorithms (Viola and Jones, 2001). To solve this problem, OBM (Li et al., 2024a) was proposed, borrowing the structure of Segment Anything Model (SAM) (Kirillov

et al., 2023). OBM was a promptable model and fully structured by Transformer, and the prompt-level offsets were predicted by Reference Offset Augmentation Module (ROAM), using a concept of offset queries. During the prompt-level test, a common pattern of predicting offsets was newly discovered, a huge performance gap between predicting longer offsets and shorter offsets, and Distance NMS algorithms were designed for solving this problem.

At this point, the BFE problem seems to be solved, and the next step for us was improving the output mask quality, simply like what has going on with SAM-HQ in general computer vision (Ke et al., 2024). Yet the effectiveness of this more intuitive experiments has not been accepted via our experiments. To make the output of the model more in line with the results of data production, which have clear vectorized boundaries and vertices, we proposed OBMv2 in this paper.

OBMv2 is a model supporting both modes of prompting and end-to-end. To get building vertex map for each prompt, an additional segmentation task is included. Within the training of this task, a new loss function, Dynamic Scope Binary Cross Entropy Loss (DS-BCE Loss), was proposed for vertex tasks. This loss function can weaken the grid effect of output results. The common pattern of predicting offset discovered by Li et al. (2024a) is newly solved with a Self Offset Attention (SOFA) layer purposely designed for offsets. SOFA was designed via Nadaraya-Watson Regression (Nadaraya, 1964; Watson, 1964). With the help of SOFA, OBMv2 can directly predict footprint vertices without post-processing algorithms like DNMS and NMS. This module can also be applied in both end-to-end and prompting model.

On the other hand, a promptable model commonly has a problem on how to squeeze knowledge in the model with external knowledge, like Retrieval-Augmented Generation (RAG) (Gao et al., 2023; Lewis et al., 2020) in Nature Language Processing. In BFE problem, we designed BFE’s RAG in two aspects: how to get better prompts; and how to squeeze knowledge on final results. The first aspect can be considered as getting auto prompts from Proposal Network. To this end, inputting all human labelled prompts can consider as the most efficient but consuming methods for prompting compared with using Proposal Network. In other words, human prompting was the ceiling of models can reach, and auto-prompting mode was attempts on how to approach the ceiling.

For the second aspect, we are inspired by The Law of Geography (Zhu et al., 2018): in spatial representation, the information contained is redundant. In fact, BFE problem can be defined by each two of building segmentation, roof segmentation, offset prediction and facade segmentation, as shown in Fig.1.

In summary, the contributions of this paper are as follows:

- OBMv2 can extract polygonal building footprint in both prompting and automatic mode. The process of extract footprint can be divided into vertex task and offset task. We designed Dynamic Scope Binary Cross Entropy Loss (DS-BCE Loss) for vertex task. Because of the vertex and offset, OBMv2 is the first model which can directly predict polygonal footprint results via vector operation.
- Self Offset Attention (SOFA) was proposed to improve offset prediction, which was applicable as a layer for other kinds of offset-based models, such as LOFT. SOFA block is a learnable module designed based on understandable real-world features, which is a successful case of combining remote sensing experience with machine learning.
- We discussed the multiplicity of solutions for BFE problems via different building-related information and integrated with other roof related models. Then, three methods for solving BEF problem were provided based on utilizing spatial correlation. Based on these experiments, we found that building segmentation tasks combined with offset are sometimes more suitable for extracting footprints. Finally, we discussed and concluded such problems as "RAG problem in BFE" to emphasize the meaning of explore promptable BFE models.

2. Related work

OBMv2 is a multi-task network based on SAM (Kirillov et al., 2023), involving prompt segmentation, polygon extraction and offset learning. SOFA block is designed based on Nadaraya-Watson regression and attention mechanism. Then, this paper explores the multi solution of BFE, based on existing geometric relationships and geographical knowledge, and interative methods to achieve better performance. In following subsections, we will introduce

other application of SAM, polygon building extraction and building offset related works to demonstrate the novelty of OBMv2.

2.1. Segment Anything Model and its Application

SAM (Kirillov et al., 2023) is a foundation model for segmentation which supports segmentation with point, bounding boxes and segmantic prompts. Ravi et al. (2024) proposed SAM 2 for promptable image and video segmentation. Compared with SAM, SAM 2 has faster inference speed and better accuracy on image and video tasks. Point to Prompt (P2P) (Guo et al., 2024) based on SAM can transform point supervision to fine visual prompt via a two-stage interable refinement process. GaussianVTON (Chen et al., 2024b) emploied a model based on SAM in post-editing view image after face refinement. SAM-HQ (Ke et al., 2024) implemented deconvolution blocks to improve the quality of image embeddings of SAM. OBM (Li et al., 2024a) proposed offset tokens and ROAM structure allows SAM to extract footprint masks.

In this paper, OBMv2 combines the idea of SAM-HQ to provide high quality semantic prompts realized automatic extraction. Additionally, OBMv2 use a newly proposed vertex tokens to extract roof key points.

2.2. Polygonal mapping of buildings

Polygonal mapping of buildings refers to extract vectorized building instances, which are accurate representations of building edges. Douglas and Peucker (1973) proposed Douglas-Peucker simplification serial techniques, but those results of these algorithms are usually rough and cannot represent the high quality edge of buildings. Wei et al. (2019) proposed refine strategies using empirical building shapes. Girard et al. (2021) using Frame-Field to align the extracted fields with ground truth contours. Zorzi et al. (2021) descibe all building polygons in a same image as an undirected graph, and then connecting detected vertices. Hisup (Xu et al., 2023) studied the issue of mask reversibility to solve polygonal mapping of buildings. They use deep convolutional neural netwrks for vertex extraction and then connecting vertices by tracing the boundary pixels from the predicted building segmentations.

In this paper, OBMv2 proposed vertex token to extract vertices, and connecting them with a similar strategy of Hisup. Compared with aforementioned,

OBMv2 is the first model which can extract polygonal building footprints in off-nadir images. The footprint polygons will be derived via vector operation.

2.3. Offset-based footprint extraction

Extracting building footprints with offsets relies on the similarity between roofs and footprints. Christie et al. (2020) proposed a method uses a U-Net decoder to give out image-level orientation and pixel-level height values. Then, Li et al. (2021, 2024b) proposed multi-task learning for BFE problem, which allows models to train on dataset with different labels. LOFT (Wang et al., 2023a) was proposed, which extracts building footprints in instances segmentation tasks. In this model, a building footprint is represented by a roof mask and a roof-to-footprint offset. OBM (Li et al., 2024a) is the first model which tokenized offset representation and extract building footprints with SAM.

In this paper, BFE problem was solved not only rely on offset tasks. Prior knowledges were applied to explore the possibility of using multiple information. *e.g.* how to extract building footprints with building segmentation and offsets? Or how to extract building footprints with building and roof segmentation? Finally, OBMv2 was integrated with other models to realize automatic extraction, and concluded former contexts as "RAG in BFE" to arise attention of researchers.

3. Methodology

This section describes the methodology of this study. We will first re-introduce the BFE problem in the first part. Changes of OBMv2 compared with OBM will be clarified in one section. Additionally, SOFA and MISS will be introduced in two separate sections.

3.1. Problem Statement

In an off-nadir remote sensing image I , there are N buildings represented as $\hat{B} = \{\hat{b}_1, \hat{b}_2, \dots, \hat{b}_N\}$. BFE problem is to identify all the building footprints $F = \{f_1, f_2, \dots, f_N\}$. In OBM, each \hat{b}_i will be represented by a corresponding prompt p_i , and p_i will interactively be inputted to the model with the image I . Then, the model will label out roof segmentation r_i and roof-to-footprint offset o_i . The f_i can be found via dragging the roof mask via offset in the evaluation stage.

Different from OBM, p_i in this paper can be empty and OBMv2 supports automatic prediction and can directly give out the footprint polygon. OBMv2 newly adds a roof vertex segmentation task, to extract v_i for \hat{b}_i , and re-focus on building body's segmentation b_i for MISS. In OBMv2, p_i was particularly designed to use roof related prompts, which is also different from OBM, as roof prompting in off-nadir will have less semantic overlapping.

In summary, OBMv2 additionally focused on two prompt-level segmentation and a global semantic segmentation task for prompting: (1) prompt-level roof vertex segmentation task; (2) prompt-level building segmentation; (3) roof semantic segmentation.

3.2. Self Offset Attention (SOFA)

Li et al. (2024a) noticed an interesting phenomenon in experiments: all applied model in prompt mode performed better in buildings with significant offset compared with lower buildings. Based on this prior experience, DNMS and soft DNMS were designed by Li et al. (2024a). These algorithms worked as a post-processing method to correct offsets. So, they have to use OpenCV operators¹ to process the roofs and offsets to get the final footprint masks.

In this paper, we proposed a trainable Self Offset Attention (SOFA) via Nadaraya-Watson Regression (Nadaraya, 1964; Watson, 1964) and Look-Ahead Masking (Vaswani et al., 2017) in Nature Language Processing (NLP) for aforementioned phenomenon. The diagram of SOFA was plotted in Fig.2 In machine learning, the nature of attention layer can be understood as a pooling layer. The mission of SOFA is to accumulate offset knowledge in longer offsets.

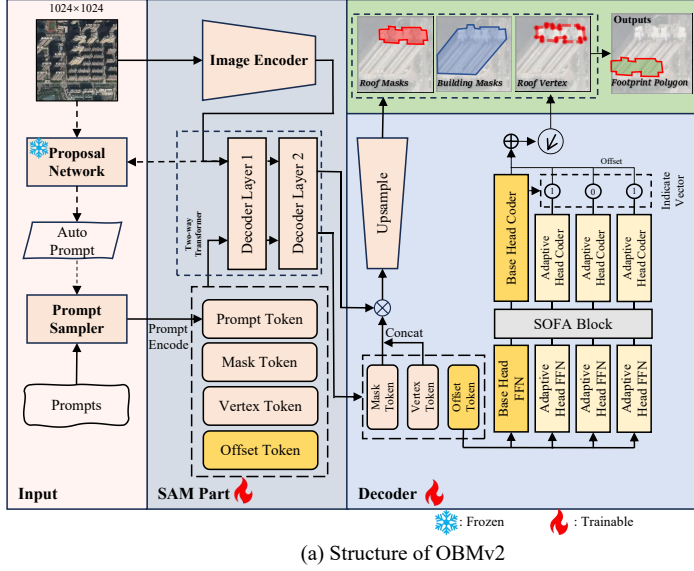
To introduce SOFA, we start with Nadaraya-Watson Kernel Regression. Nadaraya-Watson Kernel Pooling can be expressed as follows:

$$f(x) = \sum_{i=1}^n \frac{\mathcal{K}(x - x_i)}{\sum_{j=1}^n \mathcal{K}(x - x_j)} y_i \quad (1)$$

In Eq.1, f represents the Nadaraya-Watson Kernel Regression. \mathcal{K} represents kernel used in regression. If f was described in Transformer, x denotes the input *query*; $\{x_1, x_2, \dots, x_n\}$ denotes *key*; $\{y_1, y_2, \dots, y_n\}$ denotes *value*.

In BFE problem, our prior knowledge tells us: longer offsets tend to have better direction. There-

¹<https://github.com/opencv/opencv>



(a) Structure of OBMv2

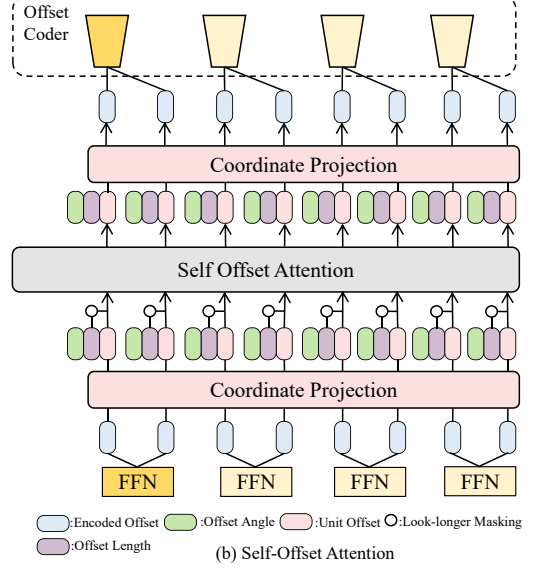


Figure 2: This figure illustrates main structures of OBMv2 and SOFA. In (a), OBMv2 newly added Proposal Networks which allow model automatically extract buildings. In prompt level, a roof vertex task was added, and the model can directly compute the location of roof vertex. Footprint polygon is calculated directly on the coordinate. SOFA structure is inserted into the original Reference Offset Augment Module (ROAM). In (b), we provide detailed SOFA block. Encoded offset once outputted from Feed Forward Network (FFN) will feed to SOFA. Then, adjusted encoded offsets will be passed to offset coders.

fore, Eq.1 is translated as Eq.2:

$$\dot{\alpha} = f(\rho, \alpha) = \sum_{i=1}^n \frac{\mathcal{K}(\rho - \rho_i)}{\sum_{j=1}^n \mathcal{K}(\rho - \rho_j)} \alpha_i \quad (2)$$

In Eq.2, offset queries $\vec{O} = \{\vec{o}_1, \vec{o}_2, \dots, \vec{o}_n\}$ was expressed as polar coordinate $\vec{O} = \{(\rho_1, \alpha_1), \dots, (\rho_n, \alpha_n)\}$. ρ means length of the offset, and α represents angle of the offset. $\dot{\alpha}$ is the corrected offset angle.

To facilitate computation, \mathcal{K} is defined as Gaussian Kernal:

$$\mathcal{K}(u) = \frac{1}{\sqrt{2\pi}} e^{(-\frac{u^2}{2})} \quad (3)$$

Consequently, Eq.2 transformed as:

$$\begin{aligned} f(\rho, \alpha) &= \sum_{i=1}^n \frac{\frac{1}{\sqrt{2\pi}} \exp\left(-\frac{(\rho - \rho_i)^2}{2}\right)}{\sum_{j=1}^n \frac{1}{\sqrt{2\pi}} \exp\left(-\frac{(\rho - \rho_j)^2}{2}\right)} \alpha_i \\ &= \sum_{i=1}^n \text{softmax}\left(-\frac{1}{2}(\rho - \rho_i)^2\right) \alpha_i \quad (4) \end{aligned}$$

To make the whole attention learnable, a trainable parameter w was added to Eq.4:

$$\begin{aligned} \dot{\alpha} &= f(\rho, \alpha) \\ &= \sum_{i=1}^n \text{softmax}\left(-\frac{1}{2}(w \times (\rho - \rho_i))^2\right) \alpha_i \quad (5) \end{aligned}$$

In NLP, look-ahead masking was used to combining the fact that tokens at one stage should only make the current and past knowledges visible for the model. Tokens in subsequent positions were masked via a huge negative number in $\text{softmax}(\cdot)$. In BFE problem, the longer offsets have better performance compared with shorter offsets. Based on aforementioned ideas, we need to design a look-longer masking \mathcal{M} for those shorter offsets. Finally, angle-level SOFA can be expressed as:

$$\begin{aligned} \dot{\alpha} &= SOFA_a(\rho, \alpha) \\ &= \sum_{i=1}^n \text{softmax}\left(-\frac{1}{2}(w \times \mathcal{M}(\rho - \rho_i))^2\right) \alpha_i \quad (6) \end{aligned}$$

Based on similar mathematical reasoning processes, vector-level SOFA can be written as:

$$\begin{aligned} \dot{\vec{o}} &= SOFA_v(\rho, \vec{u}_i) \\ &= \rho \sum_{i=1}^n \text{softmax}\left(-\frac{1}{2}(w \times \mathcal{M}(\rho - \rho_i))^2\right) \vec{u}_i \quad (7) \end{aligned}$$

\vec{u}_i is the unit offset. $\dot{\vec{o}}$ is the output offset.

From Eq.6 and Eq.7, SOFA is a portable and plug-and-play block, because (1) the learnable parameter w was light; (2) in one off-nadir image I , the number

of buildings N tend to be under 100, which makes the spatial operation of the matrix not consume much GPU memory.

3.3. Network Structure

Fig.2 (a) illustrate the proposed architecture of Offset Building Model v2 (OBMv2). OBMv2 has four new concepts compared with OBM. Firstly, Self Offset Attention block is inserted between FFN and Offset Coder ROAM structure. SOFA block provides a global awareness for each offset head and encoded offset to ensure shorter offsets can better minimize offset error. Secondly, prompt-level vertex segmentation is added in the decoder part via a vertex token. These tasks will finally be integrated with HiSup (Xu et al., 2023) to extract polygon. Thirdly, OBMv2 can receive automatic prompt from other models via a Proposal Network. Lastly, OBMv2 adopts roof-related information as prompting to reduce the adhesive relationship between buildings and achieve better differentiation of buildings.

To facilitate understanding, network structure will be detailed into three aspects: Extracting Polygonal Footprints, Proposal Network and Network Setting.

3.3.1. Extracting Polygonal Footprints

OBM is not capable of extracting polygonal footprints. To insert this function, OBMv2 using a existing roof segmentation task and a vertex segmentation task. The whole data flow was illustrated in Fig.2 (a). To begin with, a new vertex token was initialized together with mask tokens and offset tokens for each prompt. Then, these tokens will be inputted into a two-way-transformer with custom prompt token. The output of the transformer will be divided into two streams. In the mask prediction stream, vertex token will be concatenated with mask tokens; after using FFN, those tokens will divide image embeddings into roof masks, building masks and vertex masks. Using methods in HiSup, roof masks and vertex masks will finally get the simplified polygonal roofs.

In another stream, offset tokens will be passed to FFNs of ROAM structure, and the outputs of them were encoded offsets. Then, these encoded offsets will be passed into SOFA block to help them adjust themselves in a global view. The output of SOFA will be decoded as the methods of OBM. The final polygonal footprints can be calculated directly using the polygonal roofs and offsets.

3.3.2. Proposal Network

Promptable models commonly have a problem: how to activate and promote their functions. This was widely studied especially in NLP (Gao et al., 2023). As a result, proposal network was designed for automatic prompting OBMv2. The network can be defined as an instance segmentation model, semantic segmentation model or object detection model. OBMv2 provides a basic semantic segmentation head inspired by Segmenter (Strudel et al., 2021) and SAM-HQ (Ke et al., 2024). Image embeddings from image encoder will be passed to a segmenter mask transformer. The outputted image embeddings will be up-sampled $4\times$ as high quality embeddings. The these embeddings will be used to regress roofs. In this paper, more different proposal modes were applied to explore how to reach the maximum of OBMv2 in Sec.3.4.

3.3.3. Network Setting

The OBM’s losses were combined with two parts: prompt-level segmentation loss and offset losses in ROAM, which can be expressed as:

$$\mathcal{L}_{OBM} = \mathcal{L}_{ROAM} + \mathcal{L}_{roof} + \mathcal{L}_{building} \quad (8)$$

where \mathcal{L}_{ROAM} is the loss of ROAM, and SmoothL1 Loss Girshick (2015) was applied for each offset head. \mathcal{L}_{roof} is CrossEntropy Loss Shannon (1948) of roof segmentation, and $\mathcal{L}_{building}$ is CrossEntropy Loss of building segmentation.

For two new tasks, CrossEntropy Loss is applied for roof semantic segmentation. In prompt-level vertex segmentation, the model outputs a vertex map for each building. Because vertex map containing the whole scope of inputted image, this means most of the pixels will be valued as a negative sample by 0. Sparse positive keypoints will mislead the model to predict negative samples only. While via experiments, if the model uses a fixed window size to crop the building area, it can lead to severe grid effects. As a result, Dynamic Scope Binary Cross Entropy Loss (DS-BCE Loss) was designed for prompt-level vertex segmentation:

$$\mathcal{L}_{vertex} = \sum_{p \in Z + \Delta} -y_p \log y'_p - (1 - y_p) \log(1 - y'_p) \quad (9)$$

y_p and y'_p are pixels on ground truth and prediction maps located at p . Z is the original prompted area, and Δ is a random small neighborhood of this area.

Finally, OBMv2 was trained as:

$$\mathcal{L} = \lambda \times (\mathcal{L}_{OBM} + \beta \mathcal{L}_{vertex}) + \kappa \times \mathcal{L}_{seg} \quad (10)$$

λ and κ were parameters equal to 1 or 0, to control whether semantic head will be trained together. β is a scale factor to balance the loss of vertex task and other tasks.

3.4. RAG in BFE

Retrieval-Augmented Generation in NLP is a technique improving model performance with external knowledge bases (Gao et al., 2023). In BFE problem, the external knowledge can be divided into two aspects: the method of prompting and extracting footprints with multi-source results. In terms of prompting method, besides segmentation prompting, OBMv2 allows different types of prompting, including instance segmentation, object detection, *etc.* In experiments, semantic segmentation head result, LOFT (Wang et al., 2023a) results and Hybrid Task Cascade (HTC) (Chen et al., 2019) instance segmentation were tested to providing prompts for OBMv2.

Another applicable knowledge from Geography: the contained information of model results is overlapped between each other. As shown in Fig.1, there are three features, roofs, the body of buildings and building offsets, can be extracted easier than directly searching building footprints. Extracting footprints with roof segmentation and offsets is intuitive, and this method was popularly adopted in aforementioned methods. In (c), the extracting method is also explicit: move building mask along the roof-to-footprint offset, and the union between that and building mask is the footprints. Similarly, if the building mask was moved in the opposite direction, the union would be roof mask.

In (a), the situation was more complicated. The first step was to find a direction which can better represents the direction from roof to footprint. In this direction, searching algorithm was applied to detect the location of footprints by valuing different length of movements. Of course, we can also use the predicted global offset direction as this direction. In Algorithm 1, we introduced how to extract building footprint with only a roof and building segmentation. From line 1-5, a linear searching was applied to find a suitable moving angle for roof to footprint. Then, on this angle, binary searching was applied to determine the length of this moving path.

Algorithm 1 Footprint Searching

Require: Roof Segmentation: r_i , Building Segmentation: b_i , Iteration: N

Ensure: Related Footprint Segmentation: f_i

- 1: Angle list: $\alpha \leftarrow [0^\circ, 360^\circ]$
- 2: Unit Length of Offset: \bar{l}
- 3: Movements: $V = \begin{vmatrix} 1 & 0 & -\bar{l} \cos \alpha \\ 0 & 1 & -\bar{l} \sin \alpha \\ 0 & 0 & 1 \end{vmatrix}$
- 4: Moved Roofs: $\dot{R} = \{\dot{R}_1, \dot{R}_2, \dots, \dot{R}_{360}\} = V \cdot r_i$
- 5: Best Angle Value: $\theta = \arg \max_{j \in [0, 360]} S_j = \frac{\dot{R}_j \cap b_i}{r_i}$
- 6: Best Length Value:

$$l = \arg \min_{l_c} \left| \begin{vmatrix} 1 & 0 & -l_c \cos \theta \\ 0 & 1 & -l_c \sin \theta \\ 0 & 0 & 1 \end{vmatrix} \cdot r_i \cap b_i \right| - 1$$
- 7: $f_i \leftarrow$ moving r_i via θ and l

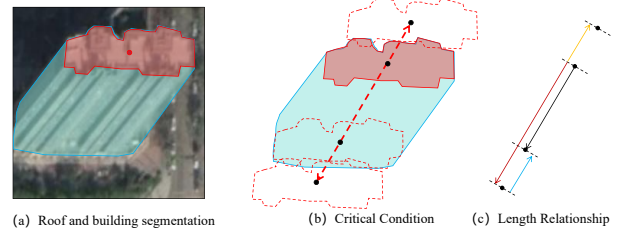


Figure 3: (a) describes the predicted roof and building for one building. (b) displays the critical condition of regressing building offset (c) abstracts the situation of (b).

When applying spatial information in Algorithm 1 to extract footprints, the Best Length Value was defined as following critical condition in Fig.3.

Fig.3(c) illustrates how to extract a more accurate offset. Aforementioned binary search was applied twice for the **yellow offset** and **red offset**. As the length of **blue offset** equal to that of the **yellow offset**. The length of roof-to-building offset is equal to the **red offset** minor the **yellow offset**.

4. Experiment and Analysis

This section describes the data used in this work, justified their choice, as well as specify their sources. Then, main results of models are reported and analyzed. Lastly, generalization test was conducted on Huizhou test set.

Table 1: Main results on BONAI (Wang et al., 2023a).

model	F1	Precision	Recall	EPE	mVL	mLL	mAL	aVL	aLL	aAL	R.IoU	R.BIoU
PANet	58.06	59.26	56.91	-	-	-	-	-	-	-	-	-
M RCNN	58.12	59.26	57.03	-	-	-	-	-	-	-	-	-
MTBR-Net	63.60	64.34	62.87	5.69	-	-	-	-	-	-	-	-
LOFT	64.42	64.43	64.41	4.85	-	-	-	-	-	-	-	-
Cas.LOFT*	62.58	63.67	61.52	4.79	-	-	-	-	-	-	-	-
MLS-BRN	66.36	65.90	66.83	4.76	-	-	-	-	-	-	-	-
p.LOFT	72.98	85.74	64.01	-	15.4	12.6	0.18	6.12	4.51	0.32	65.2	37.8
p.Cas.LOFT*	76.05	87.20	67.82	-	15.8	13.5	0.17	5.97	4.48	0.31	68.3	40.4
OBM	80.03	82.57	77.97	-	15.3	13.9	0.12	5.12	4.05	0.22	73.8	44.8
OBM [†]	78.65	80.41	77.21	-	17.0	15.7	0.12	5.38	4.35	0.22	76.5	47.9
Ours(mask)	78.74	79.85	77.91	-	17.0	15.8	0.11	5.46	4.40	0.22	77.7	50.0
Ours(poly.)	75.31	78.12	73.13	-								

Note: * model is a model that we reproduce based on the author’s intention in paper (Wang et al., 2023a). OBM[†] was retrained in roof prompting mode. p. is short for *prompt*. Additionally, R.IoU and R.BIoU represent Roof IoU and Roof Boundary IoU. PANet (Liu et al., 2018) is an instance segmentation model named Path Aggregation Network. M RCNN represents Mask RCNN(He et al., 2017). MTBR-Net (Li et al., 2021) was published on ICCV2021. LOFT (Wang et al., 2023a) was published on TPAMI2023. MLS-BRN was published on CVPR2024. EPE, mVL, mLL, aVL and aLL were in pixels. Precision, Recall, F1, R.IoU and R.BIoU were measured in percentage(%).

4.1. Dataset

In our experiments, three datasets were employed to make comparison:

(1) **BONAI** (Wang et al., 2023a): This dataset was launched with benchmark model LOFT. There are 3,000 train images and 300 test images, and the height and width of images are 1024. The annotations for buildings include roof segmentation, footprint segmentation, offset, and height.

(2) **OmniCity-view3** (Li et al., 2022): OmniCity-view3 provided 17,092 train-val images and 4,929 test images in height and width 512. Footprint segmentation, building height, roof segmentation and roof-to-footprint offset were labelled for each building.

(3) **Huizhou test set** (Li et al., 2024a): This small dataset labelled images from a new city Huizhou, China. All buildings were plotted point-to-point by human annotators. The shape of images is same with BONAI, and there are over 7,000 buildings included with offsets, roof and footprint segmentations.

On the other hand, Li et al. (2024a) also newly inserted building segmentation task for aforementioned datasets by using roof segmentations and offsets.

4.2. Metrics

In this paper, models will be reported for both prompting mode and everything mode. Promptable models adopt metrics in OBM (Li et al., 2024a) and will provide *mVL*, *mLL*, *mAL*, *aVL*, *aLL* and *aAL* to evaluate offset prediction; and offset prediction in

everything mode will be evaluated by a commonly used standard, End-point Error (EPE). For both modes, *precision*, *recall* and *f1score* are used to evaluate the final footprint prediction.

One model can support both prompting and end-to-end. In this paper, we provide a new view of valuing these model: different modes of a same model can be described as a "continuous entity". Prompting mode with accurate bounding boxes for all buildings perform as the ceiling of performance, while different auto-prompting methods and different combinations of obtained information can be seen as discrete samples for this "continuous entity". In other words, studying RAG in Remote Sensing Areas like BFE problem can benefit researchers to approach the ceiling of models.

4.3. Experimental Settings

In the training process of our OBMv2 was trained in two stages. All images will be reshaped in 1024×1024 pixels. Experiments were conducted on a server with 4 NVIDIA RTX 3090. In the first stage, OBMv2 was trained in roof prompting mode. Then, proposal networks were trained solely. In the whole training progress, we used stochastic gradient descent (SGD) (Robbins and Monro, 1951) as the optimizer with batch size of 4 for 48 epochs, and initial step learning rate of 0.0025, a momentum of 0.9, and a weight decay of 10^{-4} . The number of parameters in OBMv2 is 77.69 M.

4.4. Main Result

In this section, we evaluate our method’s on BONAI and OmniCity-view3. The main comparison will focus on LOFT (Wang et al., 2023a), Cascade LOFT and OBM between OBMv2, because these are models that available for extensive experiments. In Tab.1, the displayed results were separated into three parts. The first part lists results from end-to-end models. In the second part, all available promptable models were compared with our proposed model in part three. From this table, we know that although OBMv2 can predict offset as accurate as that of OBM in terms of direction, it suffers from incorrect length prediction. This contributes to a clear drop of footprint F1score (1.29 approximately), and a similar drop of Precision and Recall can be found in this table. Roof mask quality was surprisingly improved compared with OBM despite the drop in footprint quality. The comparison and more analysis was provided in discussion. For OBMv2, footprint F1score decreased by 3.43 during the progress of vectorizing masks. This slight decline was commonly found in experiments because polygonal footprints commonly lost those complex edges for extracting simplified features.

To ensure SOFA block is applicable in all kinds of offset-based model, the results was listed in Tab.2. In this table, a same model in both prompting mode and roof prompting was written in the same line. SOFA

Table 2: SOFA block ablation studies on BONAI.

model	EPE	mVL	mLL	mAL	aVL	aLL	aAL
LOFT	4.85	15.4	12.6	0.18	6.12	4.51	0.32
LOFT+SOFA	4.52	14.6	12.6	0.13	5.62	4.49	0.22
Cas.LOFT	4.79	15.8	13.5	0.17	5.97	4.48	0.31
Cas.LOFT+SOFA	4.43	15.3	13.4	0.12	5.64	4.44	0.22
OBM	-	15.3	13.9	0.12	5.12	4.05	0.22
OBM+SOFA	-	15.3	13.9	0.11	5.08	4.04	0.21
OBM ^T	-	17.0	15.7	0.12	5.38	4.35	0.22
OBM ^T +SOFA	-	16.8	15.7	0.11	5.36	4.35	0.21

block obviously brings gains for offset prediction. *e.g.* SOFA reduced 0.33 and 0.36 pixels’ EPE for LOFT and Cascade LOFT. mVL reduced by 0.8 pixels for prompt LOFT.

Experiments on OmniCity-view3 further demonstrate the advance of our OBMv2. In this table, OBMv2 nearly outperformed all mentioned models. Although vectorized footprint polygons still have lower F1score compared with its mask footprints, OBMv2 outperformed all mentioned models. In OBMv2, polygonal results even have better Precision compared with mask results(+0.7). Moreover, OBMv2 performed better than any other models in terms of offset prediction. aVL of OBMv2 is 1.423 pixels lower than that

Table 3: Experimental results on OmniCity-view3.

model	F1	Precision	Recall	EPE	mVL	mLL	mAL	aVL	aLL	aAL
M RCNN	69.75	69.74	69.76	-	-	-	-	-	-	-
LOFT	70.46	68.77	72.23	6.08	-	-	-	-	-	-
MLS-BRN	72.25	69.57	75.14	5.38	-	-	-	-	-	-
p.LOFT	82.27	90.63	75.81	-	54.3	48.5	0.65	7.57	5.29	0.70
p.Cas.LOFT	83.75	91.62	77.54	-	52.9	48.4	0.62	7.25	5.12	0.69
OBM	86.03	90.17	82.52	-	56.9	53.7	0.66	6.69	5.15	0.64
Ours(mask)	88.42	90.06	87.01	-	51.5	47.9	0.63	6.15	4.65	0.59
Ours(poly.)	87.61	90.76	84.93	-						

of prompt LOFT, and 0.544 pixels lower than figure for OBM. Comparing model performance we found: performance of OBMv2 on two distinct datasets was different.

In Fig.4, visulized results in prompt mode were provided. The first and second lines of illustrations were selected from BONAI(Wang et al., 2023a). The third and fouth lines were from OmniCity-view3(Li et al., 2022), and the last line was from Huizhou(Li et al., 2024a). Our model can provide polygonal results which was more editable compared with other models.

Generalization test was conducted at Huizhou test set. All models were pretrained on BONAI, and there were no extra trainings. In predicting footprints, re-

Table 4: Experimental results on Huizhou test set.

model	F1	Precision	Recall	aVL	aLL	aAL
p.LOFT	72.56	83.02	65.33	7.935	6.449	0.752
p.Cas.LOFT	75.83	81.71	71.13	7.894	5.938	0.818
OBM	81.53	78.80	84.80	4.898	4.351	0.169
OBM ^T	80.30	79.04	81.85	4.985	4.412	0.198
Ours(mask)	80.36	78.99	82.18	4.959	4.636	0.144
Ours(poly.)	75.35	77.04	74.25			

sults of OBM and OBMv2 exhibit similar attributes with them on BONAI, *e.g.* the gap between f1scores of footprints predicted by OBMv2 on BONAI(75.31) and Huizhou Test(75.35) is 0.04.

In summary, OBMv2 can directly predict footprint polygons, and the performance of which showcased a certain generalization ability. In some dataset, OBMv2 can even partially outperform aforementioned models with polygonal results. The newly proposed SOFA structure can be widely applied in different models, and bring gains for offset prediction.

4.5. RAG in BFE

Retrieval-augmented Generation (RAG) in Large Language Model emerged as a promising solution by incorporating knowledge from external databases. A similar question in BFE is how to use spatial, geosciences and prior knowledge in extracting building footprints. RAG in BFE solved problems: how to realize automatic footprint extraction and how to use

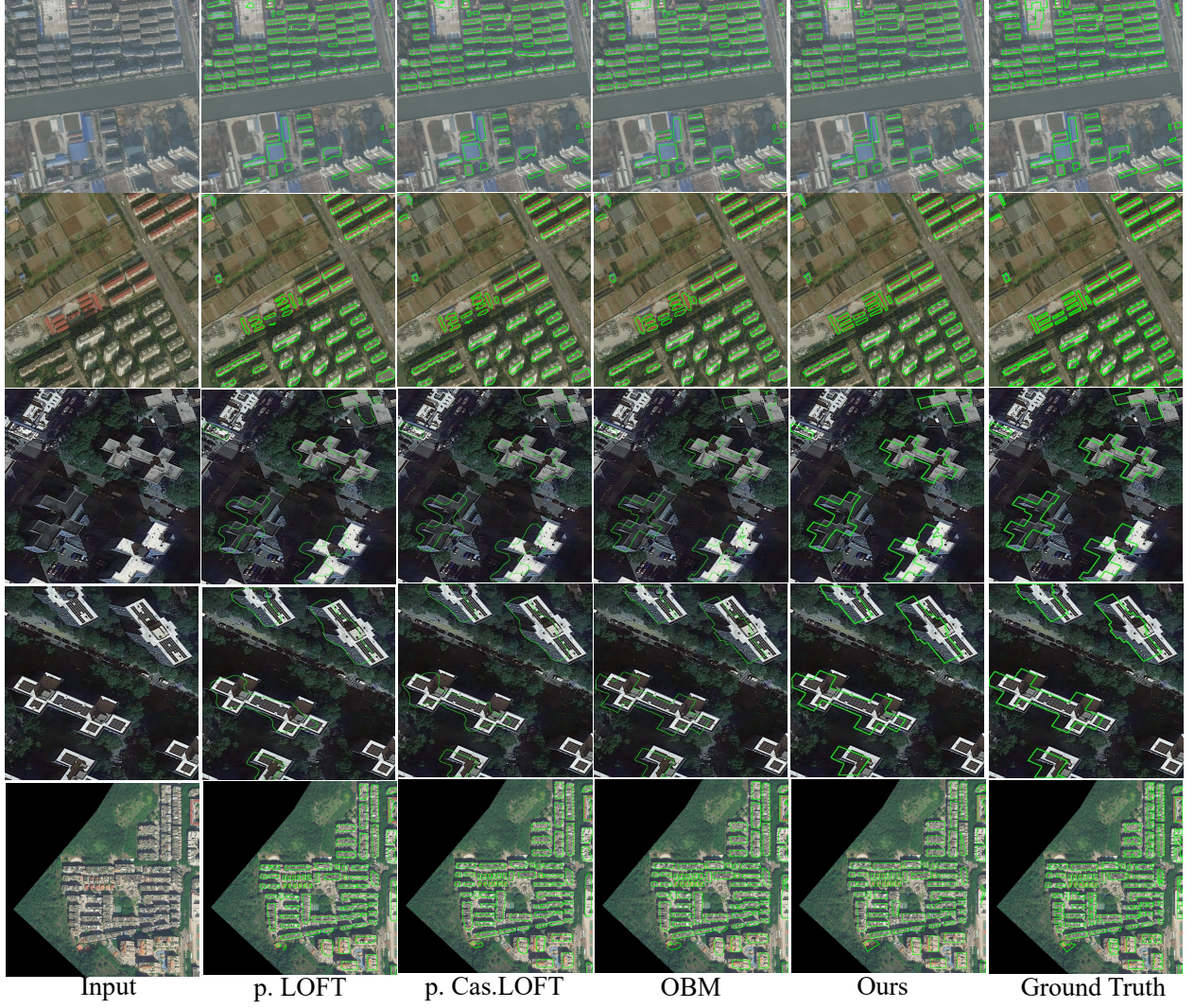


Figure 4: Main results extracted by prompting mode

different information to extract footprints. Prompting using human plotted prompts will motivate models to reach their ceiling performance. In this part, footprints f1score was selected to measure mask ability; meanwhile, EPE and aVL, which are similar in definition, were used to measure offset ability. Each model will be scattered on coordinates. To facilitate comparison, BONAI was used due to its diverse open source methods and known experimental results.

In Fig.5, BFE problem was solved by different information. For promptable models, OBM and OBMv2, building segmentation with offsets can predict better building footprint(F1score +1.37 and + 0.23 respectively). End-to-end ROI-based can also extract footprint with building segmentation and offsets, which provides similar performance with related models using roof and offset. Additionally, extracting foot-

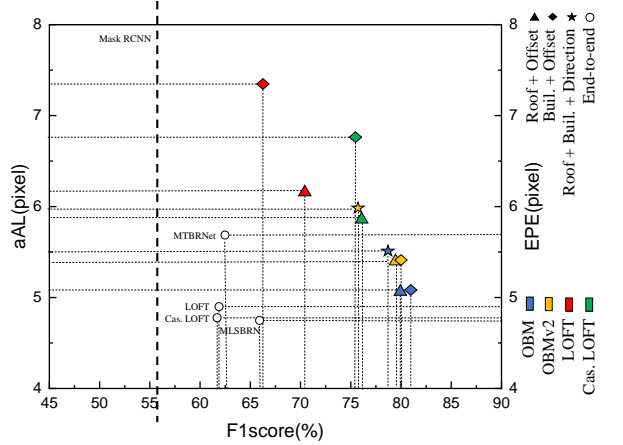


Figure 5: Extracting footprints with multi-types of information.

prints with roof and building segmentation has been proved applicable, although offsets regressed in this version was inaccurate compared with models using roofs. All models can provide better results than Mask RCNN.

The automatic extraction of building footprints commonly relies on proposal regions. In Tab.5, OBMv2 was tested with different region proposal functions. Additionally, utilizing different sources of information to extract footprint print was also examined.

Table 5: Auto extraction results on BONAI test set.

model	F1	Precision	Recall	EPE
M RCNN	56.12	57.02	55.26	-
LOFT(r.o.)	64.42	64.43	64.41	4.85
LOFT(b.o.)	61.97	61.41	62.55	5.83
Cas.LOFT(r.o.)	62.58	63.67	61.52	4.79
Cas.LOFT(b.o.)	61.67	64.59	59.00	5.23
MLS-BRN	66.36	65.90	66.83	4.76
Ours+HTC(r.o.)	61.48	55.19	74.79	-
Ours+HTC(b.o.)	61.48	55.13	74.99	4.59
Ours+seg.	55.20	64.66	50.47	-

r., b., o. and d. represent roof mask, building mask, offset and offset direction.

With the help of HTC, OBMv2 can automatically extract building footprints, and the Recall of this model is higher (+8.16) than former SOTA MLS-BRN. By adjusting different prompting mode, OBMv2 can also reach a similar Precision of MLS-BRN (-1.24).

In Fig.6, footprints extracted by auto mode were compared with each other. Our model using can still provide polygonal results compared with other models.

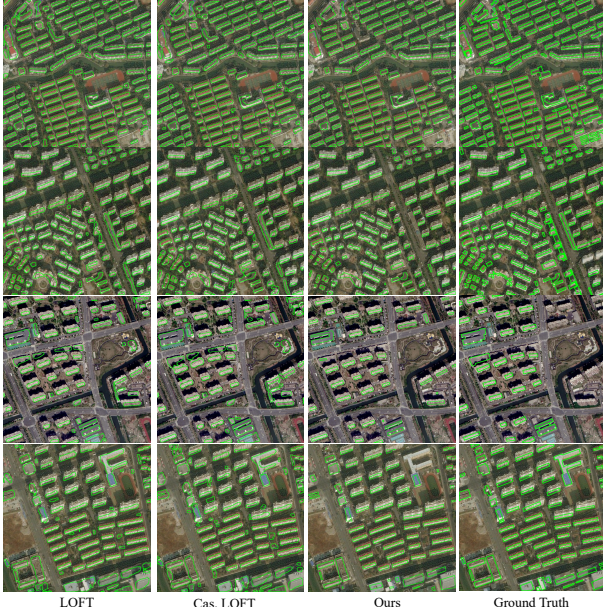


Figure 6: Main results extracted by prompting mode

5. Ablation

This section will examine the proposed algorithms and blocks. Apart from the SOFA block, aforementioned algorithms proposed for extracting footprints with different information also needs ablation.

5.1. Ablation of SOFA block

Unlike other transformer blocks, SOFA block was developed not sensitive to the input length of embedded tokens. Because of this feature, SOFA block can adapt to any offset based models. SOFA block was trained in the last stage after all other blocks finished training. In Tab.2, SOFA block was applied in all open-source models, and can reduce both prompt-level and instance-level offset error. *e.g.* EPE of LOFT on BONAI dataset declined by 0.33 pixels.

5.2. RAG in BFE: Multi-information

To ensure the proposed algorithms can extract building footprints, ablation studies were conducted with ground truth labels.

Table 6: Extract footprints with different ground truth labels on BONAI test set.

Model	F1	Precision	Recall	aVL
b.+o.	98.22	98.60	97.88	0
r.+o.	98.55	99.30	97.84	0
b.+r.	87.87	88.67	87.11	5.83
b.+r.+d.	94.37	98.17	91.69	0.67

r., b., o. and d. represent roof mask, building mask, offset and offset direction.

From Tab.6, our proposed algorithms can accurately extract building footprints via different information. Although our algorithms can extract footprints merely with roof and building segmentations, grid-based digital images always limited by image continuity. The influence of this problem is more severe especially on the representations of buildings with short offsets, *e.g.* an offset with length 1 pixel, there are only 4 points nearby can represent its end point. This ambiguity leads to poor perception of direction. As a result, when offset direction was given, the *aVL* dropped by 5.16 pixels and F1score of footprints increased by 6.5%.

5.3. RAG in BFE: Proposal Methods

OBMv2 can receive almost all kinds of models which can provide bounding boxes related to buildings. Except an extra segmentation head on OBMv2, OBMv2 was integrated with other models that can provide roof bounding boxes or segmentations. These

outputs perform as rough extraction results and OBMv2 will correct and refine them.

Table 7: Extract footprints with other roof extraction models on BONAI test set.

Model	F1	Precision	Recall	EPE
OBMv2	78.74	79.85	77.91	-
+eve	59.67	68.66	55.32	5.03
+HTC \heartsuit	61.48	55.19	74.80	4.59
+HTC \clubsuit	51.79	39.23	85.29	4.92
+HTC \clubsuit	60.70	59.18	66.32	4.42
+LOFT \heartsuit	56.24	44.01	84.33	5.07
+LOFT \clubsuit	60.26	56.32	68.48	4.59

In Tab.7, OBMv2 was integrated with its segmentation head, HTC and LOFT. Specifically, HTC and LOFT are matched with different NMS strategies. ♠ represents soft NMS algorithms with score threshold 0.05, IoU threshold 0.5, maximum 2000 instances per image. ♣ represents NMS algorithms with score threshold 0.1, IoU threshold 0.5, maximum 2000 instances per image. ♡ leverages results from ♠, but the same instance which was repeated predicted will be merged as one instance.

Soft NMS algorithm gives almost all bounding boxes with very-low score threshold. This means most output boxes will be selected as final outputs. Consequently, they can provide results with high Recall, but OBMv2 was trained with annotations can cover the whole building or roof. As a result, the Precision was not good. e.g. Precision of OBMv2 + HTC♠ is lower than that of OBMv2 + HTC♡ by 15.96%, although the Recall of OBMv2 + HTC♣ is higher than that of OBMv2 + HTC♡ by 10.49%. Finally, F1score of OBMv2 + HTC♣ was adversely influenced which only reach 51.79%.

6. Discussion

6.1. Why named "RAG in BFE"?

Prompting methods play a key role of model performance. e.g. contrastive Language-Image Pre-training (CLIP) was trained on over 400 million pairs of images and text (Radford et al., 2021). When researchers conducting experiments on classifying ImageNet (Deng et al., 2009). Researchers found using a prompt template "A photo of a {label}" can directly improve the accuracy by 1.3% compared with using a single category word "{label}". In the zone of video recognition, FineCLIPER (Chen et al., 2024a) using re-generated video captions for facial activities also improves the quality of model. In BFE problem, Li et al. (2024a)

discovered slightly larger building prompts can extract better footprints compared with those fully fitting box prompts.

RAG in LLM was another key tool which can improve the final generated results (Lewis et al., 2020). e.g. Query2doc (Wang et al., 2023b) use pseudo-documents prompting and concatenates them with the original query to improve predicting quality. Apart from the mentioned, RAG can also update knowledge and utilize external resources.

BFE problem solved by a promptable model like OBMv2 must also consider those similar problems. Except Fig.5 and Tab.7, there must be more interesting methods which help the model reaching and exceeding "the ceiling performance of using Ground Truth prompts".

6.2. Limitations of OBMv2

Limitations of OBMv2 mainly generated in two streams: the limited interactive visual zone and the training methods. OBM2 was prompted by roof. Roof prompts make the attention of OBMv2 excessively focused on the zone of "the building top". Thus, multi-attentions are less likely noticed the features in other parts of a building, although two-way transformer helps OBMv2 reference features from other buildings.

On the other hand, OBMv2 was trained with noised ground truth boxes, and these boxes can cover all pixels of each roof. However, bounding boxes which were received by OBMv2 tend to only cover a small pitch of one building, when integrating with other models, as shown in Fig.7. For such box prompts, OBMv2 cannot predict accurate offsets. Then, corresponding roofs were consequently moved to wrong places because of the uncertainty. That is why in Tab.7 soft NMS has high recall but low precision.

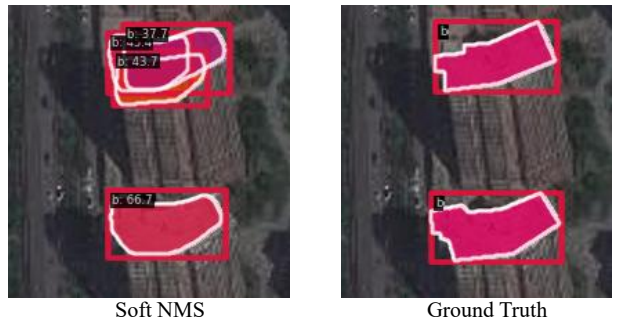


Figure 7: Some mistake samples of roof extraction made by HTC and Ground Truth label

6.3. The benefit of building task

Considering building related information was one of the contributions in this paper. For OBM and OBMv2, using building segmentation and offset robustly improves the quality of extracted footprints. To find an explanation for this, we carefully analyzed results of predicted roof and building segmentation. We found that the edge of roof and building facade is not that obvious compared with the edge between the building and background in one remote sensing image. Fig.8 displayed some typical samples which pre-

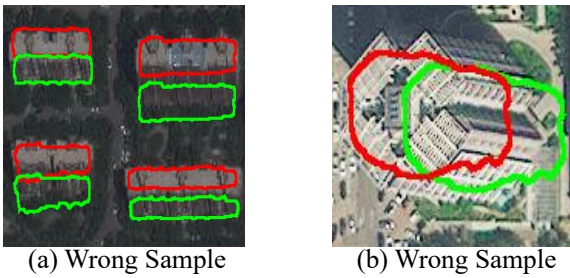


Figure 8: Some mistake samples of roof extraction

dict false roofs because of the "edge problem". Low roof quality but relatively correct offsets finally leads to a poor quality footprint. Aforementioned situation can be improved by using building segmentation like Fig.1(c).

6.4. Why OBMv2 not always outperform other models?

OBMv2 is not always better than other models. *e.g.* On BONAI (Wang et al., 2023a), OBMv2 partially outperform OBM in Tab.1, but experiments on OmniCity (Li et al., 2022) showcase the ability of OBMv2. From Fig.4, we speculate that this is likely due to the different pixel proportions occupied by buildings in the same image. The image embeddings from ViT encoder is downsampled by $16\times$. This downsampling process will adversely influence the quality of embeddings, especially when objects in images only occupied a small number of pixels. Unfortunately, this feature is very obvious on BONAI compared it on OmniCity.

6.5. Future work

Although OBM and OBMv2 outperform other end-to-end models in prompt mode, their automatic mode still cannot touch their ceiling performance. The future exploration may focus on how to tap into the

models potential like RAG in LLM. On the other hand, except BONAI(Wang et al., 2023a) and OmniCity(Li et al., 2022), there are little valid data to fine-tune models. However, many of current developed models need a vast of data to train or fine-tune. As a result, we advocate more teams to democratize their data.

7. Conclusion

This paper provides a model which can extract polygonal building footprints automatically and interactively. Because the footprint extraction is computed in vertex, this model realized end-to-end footprint extraction. This model performs better on some datasets compared with other models. For the common pattern of predicting roof-to-footprint offset, Self Offset Attention (SOFA) was designed to correct short offsets in our model. Then, this paper discussed how to use multiple information to predict footprints, and how to better integrate with other models to extract building footprints automatically. By making comparison with natural language processing, both topics were concluded as "RAG in BFE". BFE problem can be solved in different views, using building segmentation and offset can cleverly avoid the problem of unclear edges between the roof and facade.

References

- Chen, H., Huang, H., Dong, J., Zheng, M., Shao, D., 2024a. Fineclipper: Multi-modal fine-grained clip for dynamic facial expression recognition with adapters. arXiv preprint arXiv:2407.02157.
- Chen, H., Huang, Y., Huang, H., Ge, X., Shao, D., 2024b. Gaussianvton: 3d human virtual try-on via multi-stage gaussian splatting editing with image prompting. arXiv preprint arXiv:2405.07472.
- Chen, K., Pang, J., Wang, J., Xiong, Y., Li, X., Sun, S., Feng, W., Liu, Z., Shi, J., Ouyang, W., Loy, C. C., Lin, D., 2019. Hybrid task cascade for instance segmentation. In: IEEE Conf. Comput. Vis. Pattern Recog.
- Christie, G., Abujder, R. R. R. M., Foster, K., Hagstrom, S., Hager, G. D., Brown, M. Z., 2020. Learning geocentric object pose in oblique monocular images. In: Proceedings of the IEEE/CVF Conference on Computer Vision and Pattern Recognition. pp. 14512–14520.
- Deng, J., Dong, W., Socher, R., Li, L.-J., Li, K., Fei-Fei, L., 2009. Imagenet: A large-scale hierarchical image database. In: IEEE Conf. Comput. Vis. Pattern Recog. pp. 248–255.
- Douglas, D. H., Peucker, T. K., 1973. Algorithms for the reduction of the number of points required to represent a digitized line or its caricature. Cartographica: the international journal for geographic information and geovisualization 10 (2), 112–122.

Gao, Y., Xiong, Y., Gao, X., Jia, K., Pan, J., Bi, Y., Dai, Y., Sun, J., Wang, H., 2023. Retrieval-augmented generation for large language models: A survey. arXiv preprint arXiv:2312.10997.

Girard, N., Smirnov, D., Solomon, J., Tarabalka, Y., 2021. Polygonal building extraction by frame field learning. In: 2021 IEEE/CVF Conference on Computer Vision and Pattern Recognition (CVPR). pp. 5887–5896.

Girshick, R., 2015. Fast r-cnn. In: Int. Conf. Comput. Vis. pp. 1440–1448.

Guo, G., Shao, D., Zhu, C., Meng, S., Wang, X., Gao, S., 2024. P2p: Transforming from point supervision to explicit visual prompt for object detection and segmentation. IJCAI.

He, K., Gkioxari, G., Dollár, P., Girshick, R., 2017. Mask R-CNN. In: Int. Conf. Comput. Vis. pp. 2980–2988.

Inglaida, J., 2007. Automatic recognition of man-made objects in high resolution optical remote sensing images by SVM classification of geometric image features. ISPRS J. Photogramm. Remote Sens. 62 (3), 236–248.

Ke, L., Ye, M., Danelljan, M., Tai, Y.-W., Tang, C.-K., Yu, F., et al., 2024. Segment anything in high quality. Adv. Neural Inform. Process. Syst. 36.

Khattak, S. R., Buckstein, D. S., Hogue, A., 2013. Reconstructing 3d buildings from lidar using level set methods. In: 2013 International Conference on Computer and Robot Vision. pp. 151–158.

Kirillov, A., Mintun, E., Ravi, N., Mao, H., Rolland, C., Gustafson, L., Xiao, T., Whitehead, S., Berg, A. C., Lo, W.-Y., et al., 2023. Segment anything. In: Int. Conf. Comput. Vis. pp. 4015–4026.

Kunwar, S., Chen, H., Lin, M., Zhang, H., D’Angelo, P., Cerra, D., Azimi, S. M., Brown, M., Hager, G., Yokoya, N., Hänsch, R., Le Saux, B., 2021. Large-scale semantic 3-d reconstruction: Outcome of the 2019 ieee grss data fusion contest—part a. IEEE Journal of Selected Topics in Applied Earth Observations and Remote Sensing 14, 922–935.

Lafarge, F., Descombes, X., Zerubia, J., Pierrot-Deseilligny, M., 2010. Structural approach for building reconstruction from a single DSM. IEEE Trans. Pattern Anal. Mach. Intell. 32 (1), 135–147.

Lewis, P., Perez, E., Piktus, A., Petroni, F., Karpukhin, V., Goyal, N., Küttler, H., Lewis, M., Yih, W.-t., Rocktäschel, T., Riedel, S., Kiela, D., 2020. Retrieval-augmented generation for knowledge-intensive nlp tasks. In: Larochelle, H., Ranzato, M., Hadsell, R., Balcan, M., Lin, H. (Eds.), Advances in Neural Information Processing Systems. Vol. 33. Curran Associates, Inc., pp. 9459–9474.

Li, K., Deng, Y., Kong, Y., Liu, D., Chen, J., Meng, Y., Ma, J., 2024a. Prompt-driven building footprint extraction in aerial images with offset-building model.

Li, W., Lai, Y., Xu, L., Xiangli, Y., Yu, J., He, C., Xia, G.-S., Lin, D., 2022. Omnicity: Omnipotent city understanding with multi-level and multi-view images. arXiv e-prints, arXiv:2208.

Li, W., Meng, L., Wang, J., He, C., Xia, G.-S., Lin, D., 2021. 3d building reconstruction from monocular remote sensing images. In: Int. Conf. Comput. Vis. pp. 12548–12557.

Li, W., Yang, H., Hu, Z., Zheng, J., Xia, G.-S., He, C., 2024b. 3d building reconstruction from monocular remote sensing images with multi-level supervisions. arXiv preprint arXiv:2404.04823.

Lian, Y., Feng, T., Zhou, J., Jia, M., Li, A., Wu, Z., Jiao, L., Brown, M., Hager, G., Yokoya, N., Hänsch, R., Saux, B. L., 2021. Large-scale semantic 3-d reconstruction: Outcome of the 2019 ieee grss data fusion contest—part b. IEEE J. Sel. Topics Appl. Earth Observations Remote Sens. 14, 1158–1170.

Liu, S., Qi, L., Qin, H., Shi, J., Jia, J., June 2018. Path aggregation network for instance segmentation. In: IEEE Conf. Comput. Vis. Pattern Recog.

Nadaraya, E. A., 1964. On estimating regression. Theory Probab. Its Appl. 9 (1), 141–142.

Ortner, M., Descombes, X., Zerubia, J., 2008. A Marked Point Process of Rectangles and Segments for Automatic Analysis of Digital Elevation Models. IEEE Trans. Pattern Anal. Mach. Intell. 30 (1), 105–119.

Priestnall, G., Jaafar, J., Duncan, A., 2000. Extracting urban features from lidar digital surface models. Computers, Environment and Urban Systems 24 (2), 65–78.

Radford, A., Kim, J. W., Hallacy, C., Ramesh, A., Goh, G., Agarwal, S., Sastry, G., Askell, A., Mishkin, P., Clark, J., Krueger, G., Sutskever, I., 18–24 Jul 2021. Learning transferable visual models from natural language supervision. In: Meila, M., Zhang, T. (Eds.), Int. Conf. Mach. Learn. Vol. 139 of Proc. of Mach. Learn. Res. PMLR, pp. 8748–8763. URL <https://proceedings.mlr.press/v139/radford21a.html>

Ravi, N., Gabeur, V., Hu, Y.-T., Hu, R., Ryali, C., Ma, T., Khedr, H., Rädle, R., Rolland, C., Gustafson, L., et al., 2024. Sam 2: Segment anything in images and videos. arXiv preprint arXiv:2408.00714.

Robbins, H., Monroe, S., 1951. A stochastic approximation method. The annals of mathematical statistics, 400–407.

Shannon, C. E., 1948. A mathematical theory of communication. Bell Syst. Tech. J. 27 (3), 379–423.

Strudel, R., Garcia, R., Laptev, I., Schmid, C., October 2021. Segmenter: Transformer for semantic segmentation. In: Int. Conf. Comput. Vis. pp. 7262–7272.

Vaswani, A., Shazeer, N., Parmar, N., Uszkoreit, J., Jones, L., Gomez, A. N., Kaiser, L. u., Polosukhin, I., 2017. Attention is all you need. In: Guyon, I., Luxburg, U. V., Bengio, S., Wallach, H., Fergus, R., Vishwanathan, S., Garnett, R. (Eds.), Adv. Neural Inform. Process. Syst. Vol. 30. Curran Associates, Inc.

Viola, P., Jones, M., 2001. Rapid object detection using a boosted cascade of simple features. In: IEEE Conf. Comput. Vis. Pattern Recog. Vol. 1. pp. I–I.

Wang, J., Meng, L., Li, W., Yang, W., Yu, L., Xia, G.-S., 2023a. Learning to Extract Building Footprints From Off-Nadir Aerial Images. IEEE Trans. Pattern Anal. Mach. Intell. 45 (1), 1294–1301.

Wang, L., Yang, N., Wei, F., 2023b. Query2doc: Query expansion with large language models. In: Conf. Empirical Methods Natural Lang. Process. URL <https://openreview.net/forum?id=QH4EMvwF8I>

Watson, G. S., 1964. Smooth regression analysis. Sankhyā: The Indian Journal of Statistics, Series A, 359–372.

Wei, S., Ji, S., Lu, M., 2019. Toward automatic building footprint delineation from aerial images using cnn and regularization. IEEE Trans. Geosci. Remote Sens. 58 (3), 2178–2189.

Xu, B., Xu, J., Xue, N., Xia, G.-S., 2023. Hisup: Accurate polygonal mapping of buildings in satellite imagery with hierarchical supervision. ISPRS J. Photogramm. Remote Sens.

198, 284–296.

Zhu, A.-X., Lu, G., Liu, J., Qin, C.-Z., Zhou, C., 2018. Spatial prediction based on third law of geography. *Annals of GIS* 24 (4), 225–240.

Zorzi, S., Bittner, K., Fraundorfer, F., 2021. Machine-learned regularization and polygonization of building segmentation masks. In: *Int. Conf. Pattern Recog. IEEE*, pp. 3098–3105.